

Using Automatic Differentiation to Create a Nonlinear Reduced Order Model of a Computational Fluid Dynamic Solver

Jeffrey P. Thomas*, Earl H. Dowell†, and Kenneth C. Hall‡

Duke University, Durham, NC 27708-0300

Presented is a technique for developing a nonlinear reduced order model of a computational fluid dynamic solver. The method is based on a Taylor series expansion of a frequency domain harmonic balance computational fluid dynamic solver residual. The computational routines used to compute the matrices and tensors of the Taylor series expansion are created using automatic differentiation. A Ritz type expansion using proper orthogonal decomposition shapes is then used in the Taylor series expansion to create the nonlinear reduced order model. Results are presented and compared to a linear reduced order model for an inviscid transonic airfoil configuration.

Nomenclature

c	= Airfoil Chord
b	= Airfoil Chord/2
U_∞	= Velocity
M_∞	= Mach Number
Re_∞	= Reynolds Number
$\bar{\alpha}_0$	= Mean Angle-of-Attack
ω	= Frequency
$\bar{\omega}$	= Reduced Frequency, $\bar{\omega} = \omega c / U_\infty$
\bar{h}_1	= Unsteady Plunge Amplitude
$\bar{\alpha}_1$	= Unsteady Pitch Amplitude
\bar{c}_{m_1}	= Unsteady Moment Coefficient
\bar{p}_1	= Unsteady Pressure

I. Introduction

Computational fluid dynamic (CFD) models are becoming ever larger. Models with on the order of tens of millions of mesh points are now common. There is even talk of billion point mesh models coming into existence in the near future. Although the ability to create and solve such large and dense mesh CFD models is of great benefit in modeling flows about complex geometric configurations, very long computational run times are typically required, and this makes the use of such models impractical for a great many engineering analysis and design problems.

In response to this challenge, in recent years, substantial research has been conducted in developing reduced order models (ROMs) of high-dimensional CFD models with the goal of reducing computational times by orders of magnitude. See e.g. Dowell and Tang,¹ Dowell and Hall,² Lucia et al.,³ and Barone and Payne.⁴ These ROMs have proven to be of great value particularly for unsteady aerodynamic and aeroelastic

*Research Assistant Professor, Department of Mechanical Engineering and Materials Science, Senior Member AIAA.

†William Holland Hall Professor, Department of Mechanical Engineering and Materials Science, and Dean Emeritus, School of Engineering, Honorary Fellow AIAA.

‡Julian Francis Abele Professor and Department Chairperson, Department of Mechanical Engineering and Materials Science, Associate Fellow AIAA.

analysis. CFD model systems, which can easily be on the order of millions of degrees-of-freedom (DOF), have been reduced to systems with as few as a dozen DOFs while still retaining essentially the same accuracy as the full CFD model. See e.g. Thomas et al.^{5,6} and Lieu and Farhat.⁷

Typically, these ROMs have been constructed for linearized solvers. That is, time or frequency domain small disturbance solvers that are dynamically linearized about some nonlinear stationary background flow state, which may include nonlinear steady flow features such as shocks and boundary layers. These ROMs are of great value for aeroelastic flutter onset analysis, for example, reducing the computational times by several orders of magnitude. Much of the work in recent years by the aeroelasticity group at Duke University has been directed toward the development of ROMs for linearized frequency domain flow solvers.

The next major step in ROM development is to construct ROMs for dynamically nonlinear solvers for modeling those cases where the amplitude of the unsteady flow oscillation is large and/or large changes occur in the mean background flow. Such ROMs are essential for matched point flutter onset analysis as well as nonlinear limit cycle oscillation (LCO) analysis. These nonlinear ROMs will also be of great benefit for configuration design optimization for both steady and unsteady flows.

A. Objective

Our goal is the development of an accurate dynamically nonlinear ROM that will enable the rapid modeling of steady and unsteady aerodynamic flows and the associated fluid forces, particularly in the transonic Mach number region. Of particular interest is developing a method for rapidly determining the steady and unsteady aerodynamic forces created by large variations in steady flow parameters such as Mach number, angle-of-attack, and Reynolds number, as well as unsteady flow parameters such as unsteady frequency and unsteady plunge and/or pitch motion amplitudes, or more generally, changes in dynamic structural deformations. A complementary objective is to then couple the nonlinear ROM with a structural model for aeroelastic flutter, gust response, and LCO analysis.

B. A Brief Review of Relevant Reduced Order Modeling Literature

Beran and Silva⁸ and Lucia et al.³ have provided two excellent survey papers reviewing many of the most recent efforts of several researchers working in the creation of reduced order models. Most of the work has been based upon ROMs that use proper orthogonal decomposition (POD) modes (Loeve,⁹ Lumley,¹⁰ Berkooz et al.,¹¹ and Holmes et al.¹²) as shape vectors, however Silva et al.^{13,14,15} have pursued methods based upon Volterra Series. ROM researchers and their relevant publications include the following:

- Philip Beran's group at Wright Patterson Air Force base is active in ROM development using multi-POD methods (Anttonen et al.¹⁶), ROMs based on POD/Volterra methods (Lucia and Beran¹⁷), ROMs for limit cycle oscillation (Beran and Lucia¹⁸ and Beran et al.¹⁹), ROMs for panel response (Mortara et al.²⁰ and Lucia et al.²¹), ROMs for compressible flows (Lucia et al.,^{22,23} Lucia and Beran,²⁴ Pettit and Beran,²⁵ and Slater et al.²⁶), and ROMs for deforming grids (Anttonen et al.¹⁶).
- Walter Silva's group at NASA Langley is active in ROM development based on Volterra series (Silva¹³ and Marzocca et al.¹⁴) and state space ROMs for large CFD solvers (Silva and Bartels¹⁵).
- Paul Cizmas' group at Texas A&M University is active in ROM development for fluidized beds (Yaun et al.²⁷ and Cizmas et al.²⁸) and turbine rotor-stator interaction (Cizmas and Palacios²⁹).
- Karen Willcox's group at the Massachusetts Institute of Technology is active in ROM development for unsteady flow sensing (Willcox³⁰), Fourier Series ROM approaches (Willcox and Megretski³¹), aerodynamic data reconstruction and inverse design (Bui-Thanh et al.³²), ROMs for turbomachinery (Shapiro and Willcox³³ and Willcox et al.³⁴), and balanced model reduction and Arnoldi approaches (Willcox and Peraire³⁵ and Willcox et al.³⁶).
- Bogdon Epureanu's group at the University of Michigan is active in ROMs for limit cycle oscillations (Epureanu et al.³⁷) and ROM development for turbomachinery (Epureanu³⁸ and Epureanu et al.^{39,40,41}).
- Charbel Farhat's research group at Stanford University has recently become involved in ROM development for full aircraft configurations including the F-16 fighter (Lieu and Farhat⁷ and Lieu et al.⁴²).

- John Kim’s group at Boeing Aircraft in Seattle Washington is active in systems ID (identification based) ROMs (Kim⁴³ and Kim et al.^{44,45}), along with frequency domain ROMs (Kim⁴⁶).
- Our research group at Duke University has been quite active in linear and nonlinear ROM development for several years. Key areas of ROM research at Duke University include unsteady aerodynamic and aeroelastic ROMs (Thomas et al.^{6,5} Dowell et al.,⁴⁷ Hall et al.,⁴⁸ Florea et al.,⁴⁹ Tang et al.,⁵⁰ Dowell et al.,⁵¹ Dowell,⁵² and Romanowski et al.⁵³), along with ROMs for biological systems (Li and Dowell,⁵⁴ Tang and Dowell,⁵⁵ and Tang et al.⁵⁶), ROMs for models at the nanoscale (Dowell and Tang⁵⁷), and ROMs based on the systems identification approach (Attar and Dowell⁵⁸ and Tang et al.⁵⁹).

As will be discussed in the following, our new nonlinear reduced order model technique is based on a Taylor series expansion of the residual of a computational fluid dynamic solver in conjunction with a Ritz type expansion using proper orthogonal decomposition shapes. The idea is novel to the best of the authors’ knowledge.

II. Nonlinear ROM Methodology

Our approach is to construct a nonlinear ROM based on a Taylor series expansion of a given computational fluid dynamic solver residual in terms of the relevant model parameters. In the present case, we are using a nonlinear frequency domain harmonic balance (HB) CFD solution method created at Duke University (Hall et al.⁶⁰ and Thomas et al.⁶¹). However a time domain CFD solver could be treated using a similar approach. A unique aspect of the method is that computational routines used to compute the matrices and tensors of the Taylor series expansion are created using automatic differentiation. Then a Ritz type expansion using proper orthogonal decomposition shapes is used in conjunction with the Taylor series expansion to create the dynamically nonlinear reduced order model. A special and very attractive feature of the method is that in principle it can be implemented as a wrapper about existing CFD solvers with minimal changes to CFD solver code.

In recent years, the Duke University aeroelasticity research group has been active in the development of ROMs for linearized unsteady frequency domain computational flow solvers.^{6,5,48} That is, flow solvers capable of modeling unsteady aerodynamics as a result of infinitesimal structural motions for a fixed background (i.e. steady) flow condition. Although such methods are useful for aeroelastic flutter onset computations at fixed Mach numbers, they are not capable of treating large amplitude structural motions nor varying background flow conditions. In the following, we present a new technique for constructing a nonlinear ROM (we denote as NROM) about an existing computational fluid dynamic solver, which can then be used to model nonlinear unsteady aerodynamic effects brought about by changes in the mean background flow and finite amplitude structural motions. Results from the NROM are obtained at a much lower computational cost than directly using the nominal CFD solver. Such a NROM has the potential to be of great benefit for aerodynamic and aeroelastic sensitivity analysis and optimization.

III. Theoretical Development

In the following, we consider a compressible CFD code, which utilizes a nonlinear frequency domain harmonic balance solution procedure. The harmonic balance technique is implemented within the framework of a conventional time-domain CFD solver, and it provides an efficient method for modeling nonlinear unsteady aerodynamic effects brought about by finite amplitude structural motions of a prescribed frequency. See Hall et al.⁶⁰ and Thomas et al.⁶¹ for further details.

The HB/CFD solver can be considered as a vector residual operator of the form

$$\mathbf{N}(\mathbf{Q}, \mathbf{L}) = \mathbf{0} \tag{1}$$

where \mathbf{N} is the nonlinear vector residual operator of HB/CFD method, i.e.

$$\mathbf{N} = \left\{ \begin{array}{c} N_1 \\ N_2 \\ \vdots \\ N_{N_{DOF}} \end{array} \right\}, \tag{2}$$

and \mathbf{Q} is the discrete HB/CFD solution, i.e.

$$\mathbf{Q} = \begin{Bmatrix} Q_1 \\ Q_2 \\ \vdots \\ Q_{N_{DOF}} \end{Bmatrix}. \quad (3)$$

N_{DOF} is the number of degrees-of-freedom of the HB/CFD model. i.e. $N_{DOF} = N_{MESH} \times N_{EQNS}$. The vector \mathbf{L} represents the HB/CFD flow solver inputs, e.g. Mach number, Reynolds number, mean angle-of-attack, reduced frequency, unsteady motion amplitudes, etc. i.e.

$$\mathbf{L} = \begin{Bmatrix} M_\infty \\ Re_\infty \\ \bar{\alpha}_0 \\ \bar{\omega} \\ \bar{h}_1/b \\ \bar{\alpha}_1 \\ \vdots \\ \text{etc.} \end{Bmatrix}. \quad (4)$$

A. Nonlinear ROM Concept

We first consider a specific vector of flow solver inputs \mathbf{L}_0 , and we call the solution associated with this set of HB/CFD solver inputs \mathbf{Q}_0 . \mathbf{Q}_0 as such satisfies

$$\mathbf{N}(\mathbf{Q}_0, \mathbf{L}_0) = \mathbf{0}. \quad (5)$$

Next we consider a slightly different set of input variables, which we call \mathbf{L}_1 . Our objective is to be able to rapidly compute the new HB/CFD flow solution \mathbf{Q}_1 corresponding to \mathbf{L}_1 using reduced order modeling. i.e., without having to directly solve $\mathbf{N}(\mathbf{Q}_1, \mathbf{L}_1) = \mathbf{0}$ via the nominal HB/CFD solver.

The concept behind the Duke nonlinear ROM (NROM) approach is to first do a Taylor series expansion for $\mathbf{N}(\mathbf{Q}_1, \mathbf{L}_1)$ about $\mathbf{N}(\mathbf{Q}_0, \mathbf{L}_0)$. For each element of $\mathbf{N}(\mathbf{Q}_1, \mathbf{L}_1)$, the Taylor series expansion can be expressed as

$$\begin{aligned} N_i(\mathbf{Q}_1, \mathbf{L}_1) &= N_i(\mathbf{Q}_0, \mathbf{L}_0) \\ &+ \left. \frac{\partial N_i}{\partial Q_j} \right|_{\mathbf{Q}_0, \mathbf{L}_0} \Delta Q_j + \left. \frac{\partial N_i}{\partial L_j} \right|_{\mathbf{Q}_0, \mathbf{L}_0} \Delta L_j \\ &+ \frac{1}{2} \left. \frac{\partial^2 N_i}{\partial Q_j \partial Q_k} \right|_{\mathbf{Q}_0, \mathbf{L}_0} \Delta Q_j \Delta Q_k + \frac{1}{2} \left. \frac{\partial^2 N_i}{\partial Q_j \partial L_k} \right|_{\mathbf{Q}_0, \mathbf{L}_0} \Delta Q_j \Delta L_k + \frac{1}{2} \left. \frac{\partial^2 N_i}{\partial L_j \partial Q_k} \right|_{\mathbf{Q}_0, \mathbf{L}_0} \Delta L_j \Delta Q_k + \frac{1}{2} \left. \frac{\partial^2 N_i}{\partial L_j \partial L_k} \right|_{\mathbf{Q}_0, \mathbf{L}_0} \Delta L_j \Delta L_k \\ &+ H.O.T. \\ &= 0. \end{aligned} \quad (6)$$

where N_i is the i^{th} element of the HB/CFD residual vector \mathbf{N} ,

$$\Delta Q_j = Q_{j1} - Q_{j0}, \quad (8)$$

and

$$\Delta L_j = L_{j1} - L_{j0}. \quad (9)$$

H.O.T. denotes third and higher order Taylor series expansion terms. We currently truncate the series to second-order; however higher order terms can be retained.

Next, we assume a Ritz type expansion for $\Delta \mathbf{Q}$. That is, $\Delta \mathbf{Q}$ is expanded as

$$\Delta \mathbf{Q} = \mathbf{P} \Delta \mathbf{v} \quad (10)$$

where \mathbf{P} is a $N_{DOF} \times N_v$ matrix consisting of N_v POD shapes as column vectors (See Hall et al.⁴⁸ and Thomas et al.⁵ for further details on how POD vectors are created from flow solution snapshots). This expansion can also be written as

$$\Delta Q_j = \frac{\partial P_j}{\partial v_m} v_m. \quad (11)$$

We next let \mathbf{r} be the vector defined by

$$\mathbf{r} = \mathbf{P}^T \mathbf{N}. \quad (12)$$

Substituting the Ritz expansion (Eq. 10) into Eq. 7, and pre-multiplying by \mathbf{P}^T leads to the ROM form of the Taylor Series expansion

$$\begin{aligned} r_l(\mathbf{v}, \mathbf{L}_1) &= \frac{\partial r_l}{\partial v_m} \Big|_{\mathbf{Q}_0, \mathbf{L}_0} v_m + \frac{\partial r_l}{\partial L_j} \Big|_{\mathbf{Q}_0, \mathbf{L}_0} \Delta L_j \\ &+ \frac{1}{2} \frac{\partial^2 r_l}{\partial v_m \partial v_n} \Big|_{\mathbf{Q}_0, \mathbf{L}_0} v_m v_n + \frac{1}{2} \frac{\partial^2 r_l}{\partial v_m \partial L_k} \Big|_{\mathbf{Q}_0, \mathbf{L}_0} v_m \Delta L_k + \frac{1}{2} \frac{\partial^2 r_l}{\partial L_j \partial v_n} \Big|_{\mathbf{Q}_0, \mathbf{L}_0} \Delta L_j v_n + \frac{1}{2} \frac{\partial^2 r_l}{\partial L_j \partial L_k} \Big|_{\mathbf{Q}_0, \mathbf{L}_0} \Delta L_j \Delta L_k \\ &+ H.O.T. \\ &= 0. \end{aligned} \quad (13)$$

As noted previously, we truncate the system to second-order. i.e.

$$\begin{aligned} r_l(\mathbf{v}, \mathbf{L}_1) &= \frac{\partial r_l}{\partial v_m} \Big|_{\mathbf{Q}_0, \mathbf{L}_0} v_m + \frac{\partial r_l}{\partial L_j} \Big|_{\mathbf{Q}_0, \mathbf{L}_0} \Delta L_j \\ &+ \frac{1}{2} \frac{\partial^2 r_l}{\partial v_m \partial v_n} \Big|_{\mathbf{Q}_0, \mathbf{L}_0} v_m v_n + \frac{1}{2} \frac{\partial^2 r_l}{\partial v_m \partial L_k} \Big|_{\mathbf{Q}_0, \mathbf{L}_0} v_m \Delta L_k + \frac{1}{2} \frac{\partial^2 r_l}{\partial L_j \partial v_n} \Big|_{\mathbf{Q}_0, \mathbf{L}_0} \Delta L_j v_n + \frac{1}{2} \frac{\partial^2 r_l}{\partial L_j \partial L_k} \Big|_{\mathbf{Q}_0, \mathbf{L}_0} \Delta L_j \Delta L_k \\ &= 0. \end{aligned} \quad (14)$$

Equation 14 is the NROM system, and we use the Newton-Raphson technique to solve for \mathbf{v} . We use an automatic differentiation tool known as TAPENADE (<http://www-sop.inria.fr/tropics>) to derive the Jacobians and tensors in Eq. 14.

IV. Model Configuration

In the following, we examine a NACA 0012 airfoil section. We consider an inviscid transonic flow with a Mach number of $M_\infty = 0.75$ and mean angle-of-attack of $\bar{\alpha}_0 = 1.^\circ$. For the unsteady portion of the flow, we consider pitching about the quarter-chord for a first harmonic unsteady pitch amplitude $\bar{\alpha}_1 = 1.^\circ$ at a reduced frequency of $\bar{\omega} = 0.2$. Figure 1a shows the computational grid, and Fig. 1b shows computed mean flow Mach number contours. Thus we consider a nominal flow \mathbf{Q}_0 based on a nominal set of HB/CFD solver inputs \mathbf{L}_0 :

$$\mathbf{L}_0 = \left\{ \begin{array}{l} M_\infty = 0.75 \\ Re_\infty = \infty \\ \bar{\alpha}_0 = 1.^\circ \\ \bar{\omega} = 0.2 \\ \bar{h}_1/b = 0. \\ \bar{\alpha}_1 = 1.^\circ \end{array} \right\}. \quad (15)$$

We then consider an alternate flow \mathbf{Q}_1 based on a set of HB/CFD solver inputs \mathbf{L}_1 that are slightly different from \mathbf{L}_0 .

V. Nonlinearity of Underlying Solution

Figures 2 and 3 are presented to give the reader a sense of the level of the nonlinearity of the HB/CFD solution for the NACA 0012 airfoil configuration due to finite changes in four of the HB/CFD flow solver input variables. Each of these figures contains four subfigures, which illustrate how the change in first harmonic unsteady airfoil moment coefficient, divided by the change in a given HB/CFD flow solver input variable, varies with respect to the change in the same HB/CFD flow solver input variable. Figure 2 corresponds

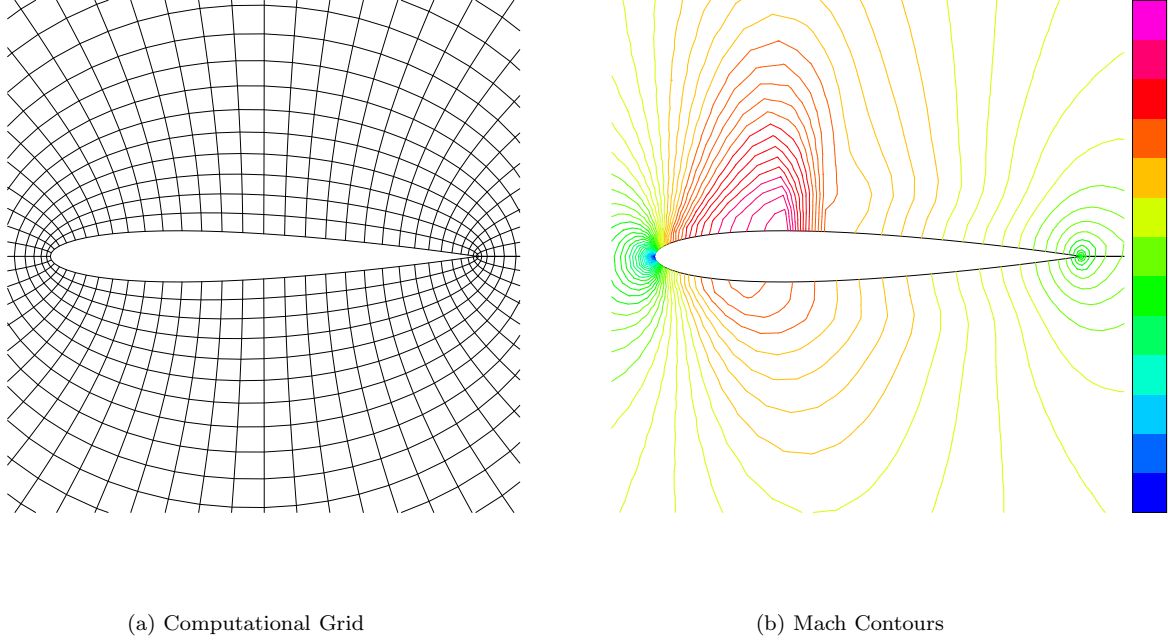


Figure 1. Computational Grid and Computed Mach Number Contours for Model NACA 0012 Airfoil Section Configuration. $M_\infty = 0.75$, $\bar{\alpha}_0 = 1.^\circ$, $\bar{\omega} = 0.2$, and $\bar{\alpha}_1 = 1.^\circ$.

to the real part of the first harmonic unsteady airfoil moment coefficient, and Fig. 3 corresponds to the imaginary part of the first harmonic unsteady airfoil moment coefficient. So for instance, Figs. 2a (real part) and 3a (imaginary part) show how the change in first harmonic unsteady airfoil moment coefficient divided by the change in HB/CFD flow solver input Mach number, varies with respect to the change in HB/CFD flow solver input Mach number. Likewise, Figs. 2b and 3b, Figs. 2c and 3c, and Figs. 2d and 3d, illustrate this same trend for changes in mean angle-of-attack, unsteady reduced frequency, and unsteady pitch amplitude, respectively. For very small changes in each of the given HB/CFD flow solver input variables (note the logarithmic scale on the abscissa of each subfigure), the ratio of the change in first harmonic unsteady airfoil moment coefficient divided by the change in a given HB/CFD flow solver input variable will be nearly constant, which indicates linear response of the HB/CFD flow solver to such small changes in the same given HB/CFD flow solver input variable. However, as soon as the change in each of the given HB/CFD flow solver input variables becomes large enough, the ratio of the change in first harmonic unsteady airfoil moment coefficient divided by the change in the same HB/CFD flow solver input variable begins to change rapidly. This indicates the magnitude at which nonlinearity of the HB/CFD solution becomes apparent for each of the HB/CFD flow solver input variables. As can be seen, Mach number changes on the order of $M_\infty - M_{\infty_0} = 0.01$, mean angle-of-attack changes on the order of $\bar{\alpha}_0 - \bar{\alpha}_{0_0} = 1.^\circ$, unsteady reduced frequency changes on the order of $\bar{\omega} - \bar{\omega}_0 = 0.1$, and unsteady pitch amplitude changes on the order of $\bar{\alpha}_1 - \bar{\alpha}_{1_0} = 1.^\circ$ all lead to significant nonlinear response of the HB/CFD flow solver solution for the NACA 0012 airfoil configuration.

VI. Nonlinear ROM Testing

In order to first test the NROM for correctness, we consider a single POD vector, which we set equal to the difference between the directly computed HB/CFD flow solver solutions for the \mathbf{L}_1 and \mathbf{L}_0 HB/CFD solver input cases. i.e. $\mathbf{P}_1 = \mathbf{Q}_1 - \mathbf{Q}_0$. Based on the NROM Ritz expansion (Eq. 10), this implies that

$$\mathbf{Q}_1 = \mathbf{Q}_0 + v_1 (\mathbf{Q}_1 - \mathbf{Q}_0), \quad (16)$$

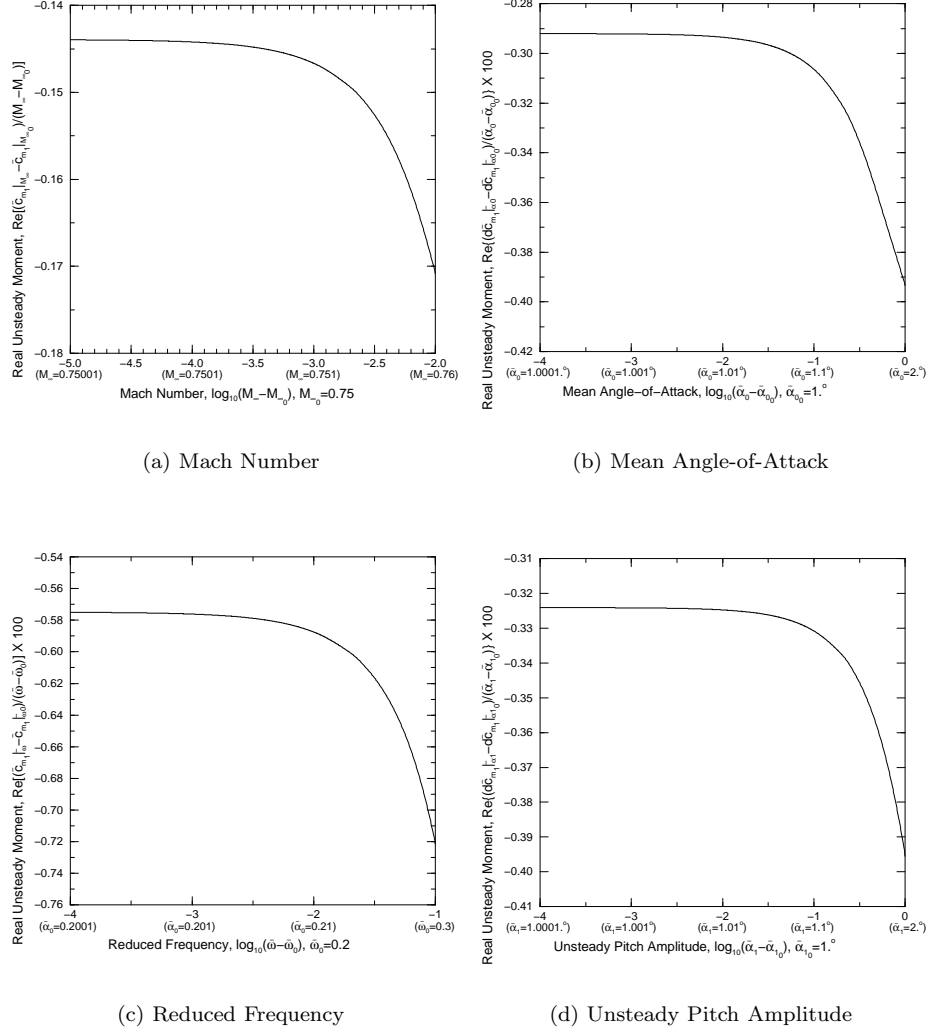


Figure 2. Real Part of Change in Unsteady Pitching Moment Coefficient with Respect to Changes in Various HB/CFD Flow Solver Inputs.

the exact solution of which is $v_1 = 1$. We next use the NROM to solve for v_1 . Two things should occur if the NROM is working correctly. First, in the limit as $\mathbf{L}_1 \rightarrow \mathbf{L}_0$, $v_1 \rightarrow 1$. Second, for larger differences between \mathbf{L}_1 and \mathbf{L}_0 , the second-order NROM results for v_1 should stay closer to one when compared to those obtained from the first-order linear ROM. This is because the NROM second-order nonlinear terms are helping to account for the nonlinear effects.

Table 1 shows the results when varying the Mach number for the first-order linear ROM and the second-order nonlinear NROM. As can be seen when compared to Figs. 2a and 3a, the first-order ROM holds up well when $M_\infty - M_{\infty_0} < 0.001$. i.e. $v_1 \approx 1$. However, when nonlinear effects become readily apparent, (i.e. $M_\infty - M_{\infty_0} > 0.001$), the second-order NROM performs much better. In fact, for a Mach number difference as high as 0.05 (and this being in the transonic Mach number flow region no less), the second-order NROM has less than one percent error compared to nearly an 11 percent error for the first-order linear ROM. We have performed similar tests for the other HB/CFD flow solver input variables, and the second-order NROM always performs better than the first-order linear ROM.

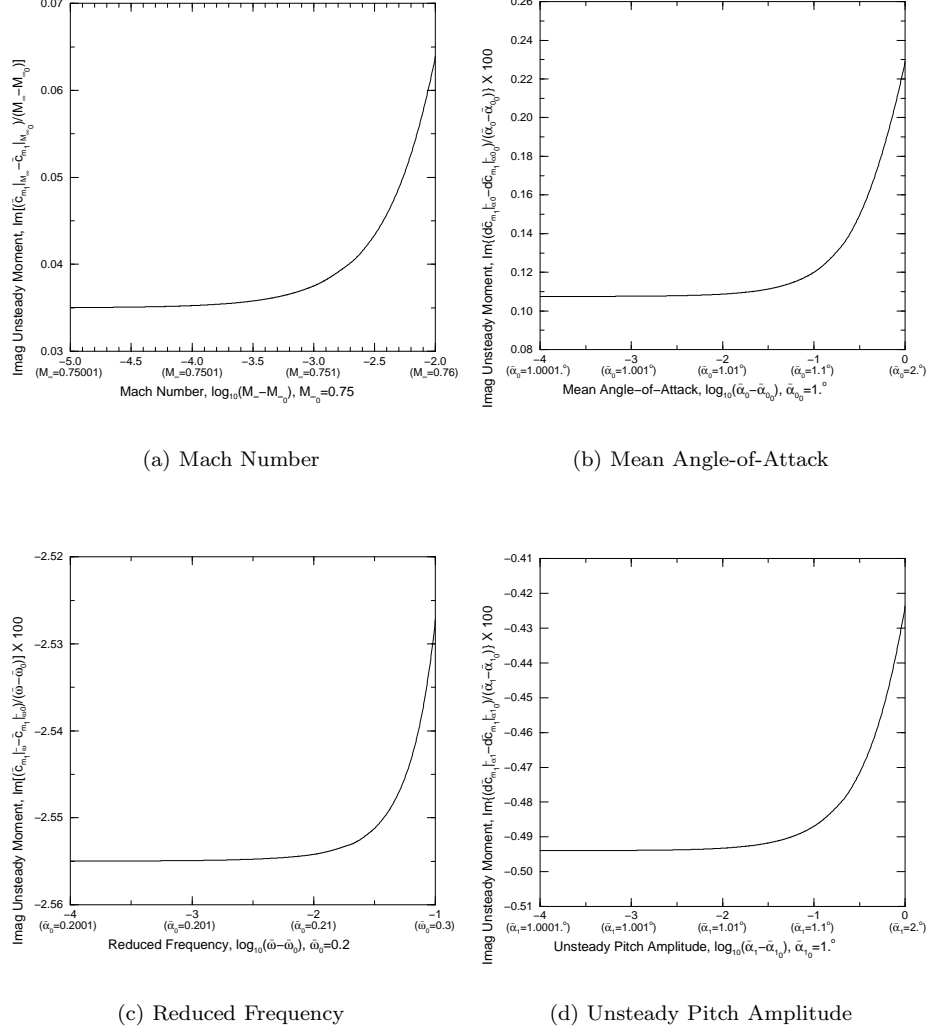


Figure 3. Imaginary Part of Change in Unsteady Pitching Moment Coefficient with Respect to Changes in Various HB/CFD Flow Solver Inputs.

VII. NROM Results When Using POD Vectors for Mach Number Variation

We next consider the case of constructing the NROM using proper orthogonal decomposition vectors. In this instance, we consider varying a single independent variable, in this case, Mach number. The POD vectors are created from a set of flow solution snapshots. The POD vectors in fact are simply a linear rearrangement of a given set of flow solution snapshots. For the case where we wish to vary Mach number in the NROM, we directly compute flow solutions of a number of discrete Mach numbers while leaving the rest of the HB/CFD flow solver independent variables unchanged. There are many possible options for the snapshots. In this case, we would like to pick snapshots within the Mach number range where nonlinear behavior is observed. As noted before, nonlinear behavior is clearly noticeable for $M_\infty - M_{\infty_0} > 0.001$. We also consider the upper Mach number difference we wish to model to be $M_\infty - M_{\infty_0} = 0.01$.

In this instance, we have computed a total of four solution snapshots for Mach numbers of $M_\infty = 0.7501$, $M_\infty = 0.751$, $M_\infty = 0.755$, and $M_\infty = 0.76$. Four POD vectors are then created from these four snapshots. At this stage, our objective is to demonstrate that the second-order NROM is more accurate than the first-order ROM when using the same POD shapes. We therefore have arbitrarily chosen solution snapshots in this case such that there are a couple of snapshots in the nearly linear response range, and a couple of

$M_\infty - M_{\infty 0}$	$\log_{10}(M_\infty - M_{\infty 0})$	1st Order ROM	2nd Order NROM
0.00001	-5.000	1.00000751459674	1.00000000192930
0.0001	-4.000	1.00007537043337	1.00000023383994
0.0005	-3.301	1.00038384256020	1.00000569085761
0.001	-3.000	1.00079473657590	1.00002169303130
0.005	-2.301	1.00639988148592	1.00016897238936
0.01	-2.000	1.01389537771078	0.999958887892929
0.05	-1.301	1.10879824566932	0.992551721939127

Table 1. ROM Results for Steady Flow Mach Number Variation - Computed Values for v_1 (Eq. 16).

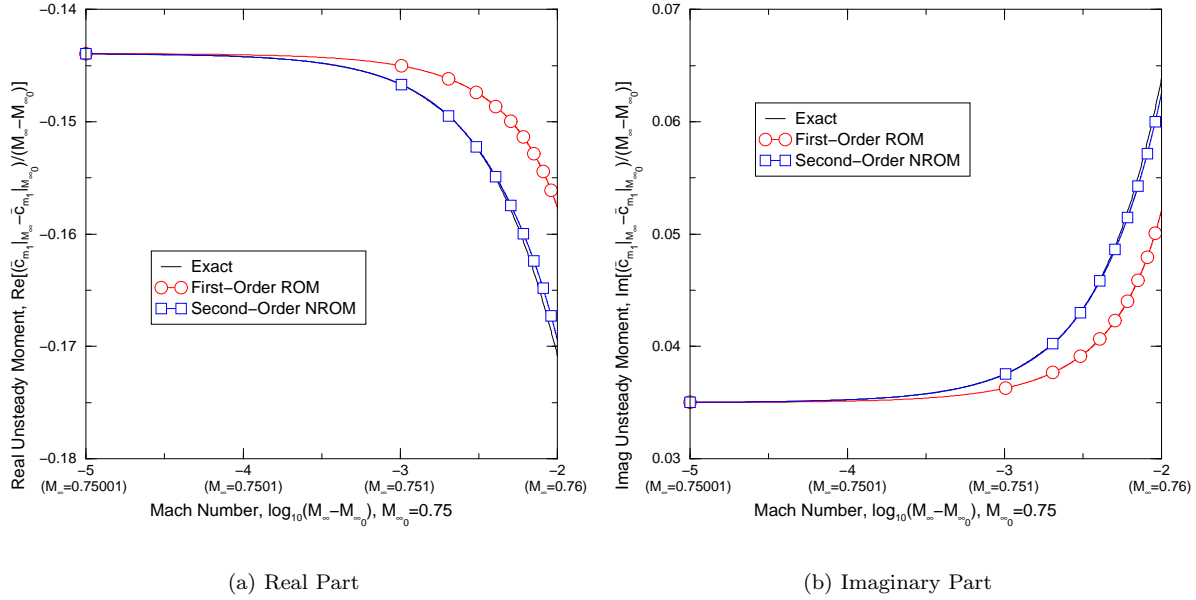


Figure 4. First-Order Linear ROM and Second-Order Nonlinear NROM Performance in Modeling the Change in Unsteady Pitching Moment Coefficient with Respect to Changes in Mach Number. $\bar{\alpha}_0 = 1.^\circ$, $\bar{\omega}_0 = 0.2$, and $\bar{\alpha}_1 = 1.^\circ$.

snapshots in the beginnings of the nonlinear response range. Note the change in first harmonic unsteady airfoil moment coefficient, divided by the change in HB/CFD flow solver input Mach number, response trend with respect to the change in HB/CFD flow solver input Mach number (See Figs. 2a and 3a). Note also, the POD shapes are just a linear rearrangement of the solution snapshots. So when we use all the available POD vectors, we could just as well use all the solution snapshots as shape vectors.

We now use the NROM with the four available POD vectors to model the results shown in Figs. 2a and 3a. Figure 4 shows the results for both the first-order ROM and second-order NROM as compared to the exact solution. As can be seen, the second-order NROM performs significantly better than the first-order ROM.

VIII. NROM Results When Varying Multiple Independent Variables

In this section, we consider the case where we vary multiple independent variables. Namely Mach number, mean angle-of-attack, unsteady reduced frequency, and unsteady pitch amplitude. We arbitrarily choose the

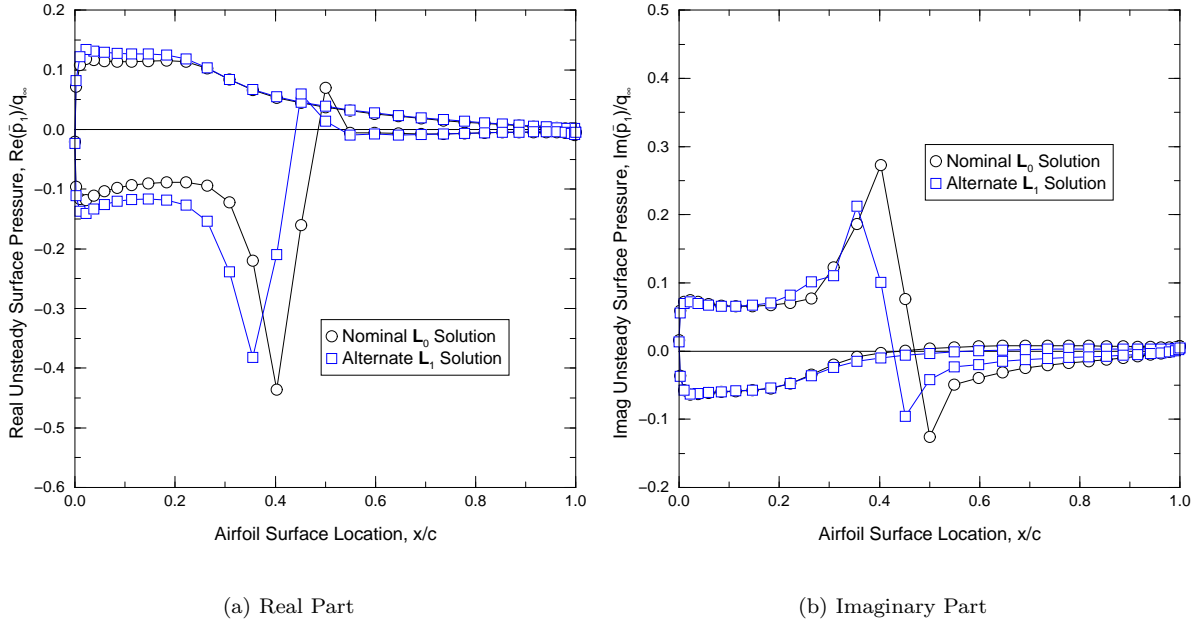


Figure 5. Difference in Unsteady Surface Pressure Distributions Between L_0 and L_1 HB/CFD Flow Solver Input Cases.

HB/CFD solver inputs L_1 to be

$$\mathbf{L}_1 = \left\{ \begin{array}{l} M_\infty = 0.7575 \\ Re_\infty = \infty \\ \bar{\alpha}_0 = 1.125^\circ \\ \bar{\omega} = 0.275 \\ \bar{h}_1/b = 0. \\ \bar{\alpha}_1 = 1.075 \end{array} \right\}. \quad (17)$$

The changes in Mach number, mean angle-of-attack, unsteady reduced frequency, and unsteady pitch amplitude between the L_1 and L_0 conditions are large enough such that nonlinear response of the HB/CFD solver is observed. In fact, Fig. 5 shows the real (Fig. 5a) and imaginary (Fig. 5b) parts of the first harmonic unsteady surface pressure for both the L_0 and L_1 HB/CFD flow solver input conditions. As can be seen, the solutions are considerably different, particularly for the shock location.

We begin by computing a set solution snapshots in order to create POD vectors. As with the Mach number variation case in the previous section, we consider four solution snapshots for Mach numbers of $M_\infty = 0.7501$, $M_\infty = 0.751$, $M_\infty = 0.755$, and $M_\infty = 0.76$. We then also consider four flow solution snapshots for mean angles-of-attack of $\bar{\alpha}_0 = 1.001^\circ$, $\bar{\alpha}_0 = 1.01^\circ$, $\bar{\alpha}_0 = 1.1^\circ$, and $\bar{\alpha}_0 = 1.2^\circ$, four flow solution snapshots for unsteady reduced frequencies of $\bar{\omega} = 0.201$, $\bar{\omega} = 0.21$, $\bar{\omega} = 0.25$, and $\bar{\omega} = 0.3$, and four flow solution snapshots for unsteady pitch amplitudes of $\bar{\alpha}_1 = 1.001^\circ$, $\bar{\alpha}_1 = 1.01^\circ$, $\bar{\alpha}_1 = 1.1^\circ$, and $\bar{\alpha}_1 = 1.2^\circ$. This results in a total of sixteen snapshots from which we create sixteen POD shapes for use in the NROM. As in the previous section, we have arbitrarily chosen solution snapshots intervals. Our objective at this stage is to demonstrate that the second-order NROM is more accurate than the first-order ROM when using the same POD shapes. Future studies will investigate if there are optimal snapshot resolutions.

Figure 6 shows the real (Fig. 6a) and imaginary (Fig. 6b) parts of the first harmonic unsteady surface pressure for the exact solution, along with first-order ROM and second-order NROM results, corresponding to the HB/CFD solver inputs L_1 . As can be seen, the second-order NROM performs significantly better than the first-order linear ROM.

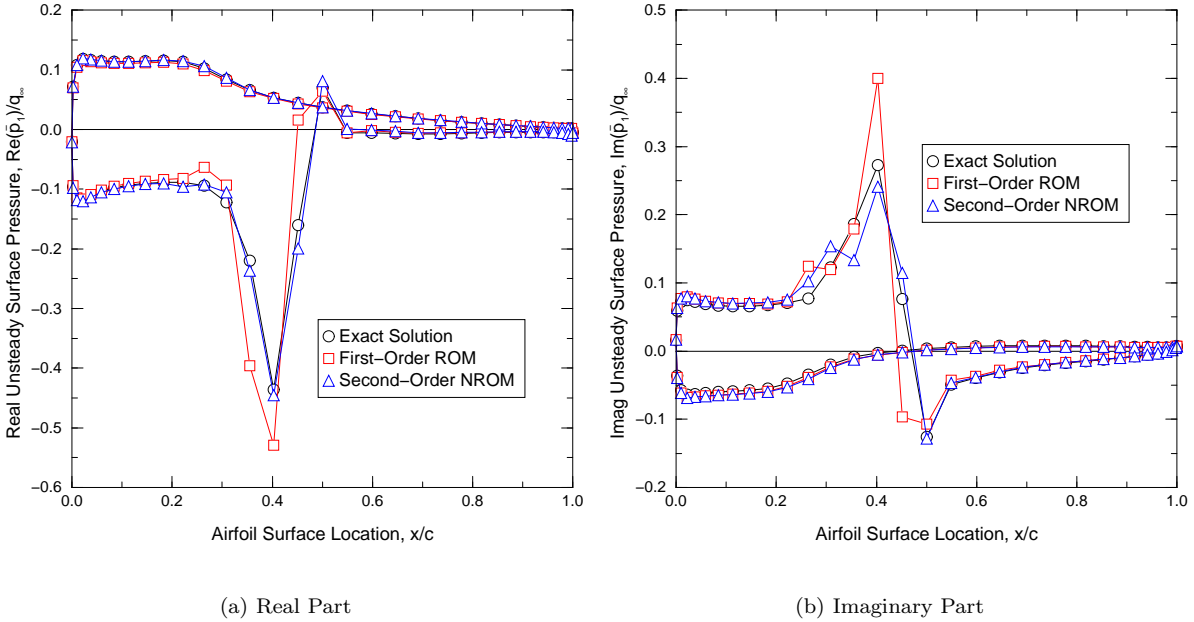


Figure 6. Linear and Nonlinear ROM Performance for Real and Imaginary Unsteady Pressure Distributions. $M_\infty = 0.7575$, $\bar{\alpha}_0 = 1.125^\circ$, $\bar{\omega} = 0.275$, and $\bar{\alpha}_1 = 1.075^\circ$.

IX. Conclusions

A method for creating a nonlinear reduced order model of a computational fluid dynamic flow solver is presented. The technique is based on a Taylor series expansion of the flow solver residual together with a Ritz type expansion using proper orthogonal decomposition shapes. Automatic differentiation is used to derive the Taylor series expansion of the fluid dynamic solver residual. Applying the method to an inviscid transonic airfoil configuration illustrates that the nonlinear reduced order model performs much better than a linear reduced order model when considering large changes in the flow solver input variables.

References

- ¹Dowell, E. H. and Tang, D. M., *Dynamics of Very High Dimensional Systems*, World Scientific Publishing Co., 2003.
- ²Dowell, E. H. and Hall, K. C., "Modeling of Fluid-Structure Interaction," *Annual Review of Fluid Mechanics*, Vol. 33, 2001, pp. 445–490.
- ³Lucia, D. J., Beran, P. S., and Silva, W. A., "Reduced-Order Modeling: New Approaches for Computational Physics," *Progress in Aerospace Sciences*, Vol. 40, No. 1–2, February 2004, pp. 51–117.
- ⁴Barone, M. F. and Payne, J. L., "Methods for Simulation-Based Analysis of Fluid-Structure Interaction," Tech. Rep. SAND2005-6573, Sandia National Lab, Albuquerque, and Livermore, California, New Mexico 87185, 2005.
- ⁵Thomas, J. P., Dowell, E. H., and Hall, K. C., "Three-Dimensional Transonic Aeroelasticity Using Proper Orthogonal Decomposition-Based Reduced-Order Models," *Journal of Aircraft*, Vol. 40, No. 3, May–June 2003, pp. 544–551.
- ⁶Thomas, J. P., Dowell, E. H., and Hall, K. C., "Static/Dynamic Correction Approach for Reduced-Order Modeling of Unsteady Aerodynamics," *Journal of Aircraft*, Vol. 43, No. 4, July–August 2006, pp. 865–878.
- ⁷Lieu, T. and Farhat, C., "Adaptation of POD-Based Aeroelastic ROMs for Varying Mach Number and Angle of Attack: Application to a Complete F-16 Configuration," AIAA Paper 2005-7666.
- ⁸Beran, P. S. and Silva, W. A., "Reduced Order Modeling: New Approaches for Computational Physics," AIAA Paper 2001-0853.
- ⁹Loeve, M., *Probability Theory*, D. Van Nostrand Company, Inc., New York, 1955.
- ¹⁰Lumley, J. L., "The Structures of Inhomogeneous Turbulent Flow," *Atmospheric Turbulence and Radio Wave Propagation*, 1967, pp. 166–178, Edited by Yaglom, A. M. and Tatarski, V. I.
- ¹¹Berkooz, G., Holmes, P., and Lumley, J. L., "The Proper Orthogonal Decomposition in the Analysis of Turbulent Flows," *Annual Review of Fluid Mechanics*, Vol. 25, 1993, pp. 539–575.
- ¹²Holmes, P., Lumley, J. L., and Berkooz, G., *Turbulence, Coherent Structures, Dynamical Systems and Symmetry*, Cambridge University Press, 1996.

- ¹³Silva, W., "Identification of Nonlinear Aeroelastic Systems Based on the Volterra Theory: Progress and Opportunities," *Nonlinear Dynamics*, Vol. 39, No. 1–2, January 2005, pp. 25–62.
- ¹⁴Marzocca, P., Silva, W. A., and Librescu, L., "Nonlinear Open-/Closed-Loop Aeroelastic Analysis of Airfoils via Volterra Series," *AIAA Journal*, Vol. 42, No. 4, April 2004, pp. 673–686.
- ¹⁵Silva, W. A. and Bartels, R. E., "Development of Reduced-Order Models for Aeroelastic Analysis and Flutter Prediction Using the CFL3Dv6.0 Code," *Journal of Fluids and Structures*, Vol. 19, No. 6, July 2005, pp. 729–745.
- ¹⁶Anttonen, J. S. R., King, P. I., and Beran, P. S., "POD-Based Reduced-Order Models with Deforming Grids," *Mathematical and Computer Modelling*, Vol. 38, No. 1–2, July 2004, pp. 41–62.
- ¹⁷Lucia, D. J. and Beran, P. S., "Reduced-Order Model Development Using Proper Orthogonal Decomposition and Volterra Theory," *AIAA Journal*, Vol. 42, No. 6, June 2005, pp. 1181–1190.
- ¹⁸Lucia, D. J. and Beran, P. S., "Aeroelastic System Development Using Proper Orthogonal Decomposition and Volterra Theory," *Journal of Aircraft*, Vol. 42, No. 2, March–April 2005, pp. 509–518.
- ¹⁹Beran, P. S., Lucia, D. J., and Pettit, C. L., "Reduced-Order Modeling of Limit-Cycle Oscillation for Aeroelastic Systems," *Journal of Fluids and Structures*, Vol. 19, No. 5, June 2004, pp. 575–590.
- ²⁰Mortara, S. A., Slater, J., and Beran, P. S., "Analysis of Nonlinear Aeroelastic Panel Response Using Proper Orthogonal Decomposition," *Journal of Vibration and Acoustics - Transactions of the ASME*, Vol. 126, No. 3, July 2004, pp. 416–421.
- ²¹Lucia, D. J., Beran, P. S., and King, P. I., "Reduced-Order Modeling of an Elastic Panel in Transonic Flow," *Journal of Aircraft*, Vol. 40, No. 2, March–April 2003, pp. 338–347.
- ²²Lucia, D. J., King, P. I., and Beran, P. S., "Domain Decomposition for Reduced-Order Modeling of a Flow with Moving Shocks," *AIAA Journal*, Vol. 40, No. 11, November 2002, pp. 2360–2362.
- ²³Lucia, D. J., King, P. I., and Beran, P. S., "Reduced Order Modeling of a Two Dimensional Flow with Moving Shocks," *Computers and Fluids*, Vol. 32, 2003, pp. 917–938.
- ²⁴Lucia, D. J. and Beran, P. S., "Projection Methods for Reduced Order Models of Compressible Flows," *Journal of Computational Physics*, Vol. 188, No. 1, June 2003, pp. 252–280.
- ²⁵Pettit, C. L. and Beran, P. S., "Application of Proper Orthogonal Decomposition to the Discrete Euler Equations," *International Journal for Numerical Methods in Engineering*, Vol. 55, No. 4, October 2002, pp. 479–497.
- ²⁶Slater, J. C., Pettit, C. L., and Beran, P. S., "In-situ Residual Tracking in Reduced Order Modeling," *Journal of Shock and Vibration*, Vol. 9, No. 3, 2002, pp. 105–121.
- ²⁷Yuan, T., Cizmas, P. G., and O'Brien, T., "A Reduced-Order Model for a Bubbling Fluidized Bed Based on Proper Orthogonal Decomposition," *Computers & Chemical Engineering*, Vol. 30, No. 2, December 2005, pp. 243–259.
- ²⁸Cizmas, P. G., Palacios, A., O'Brien, T., and Syamlal, M., "Proper-Orthogonal Decomposition of Spatio-Temporal Patterns in Fluidized Beds," *Chemical Engineering Science*, Vol. 58, No. 19, October 2003, pp. 4417–4427.
- ²⁹Cizmas, P. G. and Palacios, A., "Proper Orthogonal Decomposition of Turbine Rotor-Stator Interaction," *Journal of Propulsion and Power*, Vol. 19, No. 2, March–April 2003, pp. 268–281.
- ³⁰Willcox, K., "Unsteady Flow Sensing and Estimation via the Gappy Proper Orthogonal Decomposition," *Computers and Fluids*, Vol. 35, No. 2, February 2006, pp. 208–226.
- ³¹Willcox, K. and Megretski, A., "Fourier Series for Accurate, Stable, Reduced-Order Models in Large-Scale Linear Applications," *SIAM Journal on Scientific Computing*, Vol. 26, No. 3, 2005, pp. 944–962.
- ³²Bui-Thanh, T., Damodaran, A., and Willcox, K., "Aerodynamic Data Reconstruction and Inverse Design Using Proper Orthogonal Decomposition," *AIAA Journal*, Vol. 42, No. 8, August 2004, pp. 1505–1516.
- ³³Shapiro, B. and Willcox, K. E., "Analyzing Mistuning of Bladed Disks by Symmetry and Reduced-Order Aerodynamic Modeling," *Journal of Propulsion and Power*, Vol. 19, No. 2, March–April 2003, pp. 307–311.
- ³⁴Willcox, K., Peraire, J., and Paduano, J. D., "Application of Model Order Reduction to Compressor Aeroelastic Models," *Journal of Engineering for Gas Turbines and Power - Transactions of the ASME*, Vol. 124, No. 2, April 2002, pp. 332–339.
- ³⁵Willcox, K. and Peraire, J., "Balanced Model Reduction Via the Proper Orthogonal Decomposition," *AIAA Journal*, Vol. 40, No. 11, November 2002, pp. 2323–2330.
- ³⁶Willcox, K., Peraire, J., and White, J., "An Arnoldi Approach for Generation of Reduced-Order Models for Turbomachinery," *Computers and Fluids*, Vol. 31, No. 2, March 2001, pp. 369–389.
- ³⁷Epureanu, B. I. and Dowell, E. H., "Compact Methodology for Computing Limit-Cycle Oscillations in Aeroelasticity," *Journal of Aircraft*, Vol. 40, No. 5, September–October 2003, pp. 955–963.
- ³⁸Epureanu, B. I., "A Parametric Analysis of Reduced Order Models of Viscous Flows in Turbomachinery," *Journal of Fluids and Structures*, Vol. 17, No. 7, 2003, pp. 971–982.
- ³⁹Epureanu, B. I., Dowell, E. H., and Hall, K. C., "Mach Number Influence on Reduced-Order Models of Inviscid Potential Flows in Turbomachinery," *Journal of Fluids Engineering*, Vol. 124, 2002, pp. 977–987.
- ⁴⁰Epureanu, B. I., Hall, K. C., and Dowell, E. H., "Reduced Order Models in Turbomachinery Using Inviscid-Viscous Coupling," *Journal of Fluids and Structures*, Vol. 15, No. 2, 2001, pp. 255–276.
- ⁴¹Epureanu, B. I., Dowell, E. H., and Hall, K. C., "Reduced-Order Models of Unsteady Transonic Viscous Flows in Turbomachinery," *Journal of Fluids and Structures*, Vol. 14, No. 8, November 2000, pp. 1215–1234.
- ⁴²Lieu, T., Farhat, C., and Lesoinne, M., "POD-based Aeroelastic Analysis of a Complete F-16 Configuration: ROM Adaptation and Demonstration," *AIAA Paper 2005-2295*.
- ⁴³Kim, T., "Efficient Reduced-Order System Identification for Linear Systems with Multiple Inputs," *AIAA Journal*, Vol. 43, No. 7, July 2005, pp. 1455–1464, 2005.
- ⁴⁴Kim, T., Hong, M., Bhatia, K. G., and SenGupta, G., "Aeroelastic Model Reduction for Affordable Computational Fluid Dynamics-Based Flutter Analysis," *AIAA Journal*, Vol. 43, No. 12, December 2005, pp. 2487–2495.
- ⁴⁵Kim, T., Nagaraja, K. S., and Bhatia, K. G., "Order Reduction of State-Space Aeroelastic Models Using Optimal Modal Analysis," *Journal of Aircraft*, Vol. 41, No. 6, November–December 2004, pp. 1440–1448.

- ⁴⁶Kim, T., "Frequency-Domain Karhunen-Loeve Method and Its Application to Linear Dynamic Systems," *AIAA Journal*, Vol. 36, No. 11, November 1998, pp. 2117–2123.
- ⁴⁷Dowell, E. H., Thomas, J. P., and Hall, K. C., "Transonic Limit Cycle Oscillation Analysis Using Reduced Order Aerodynamic Models," *Journal of Fluids and Structures*, Vol. 19, No. 1, 2004, pp. 17–27.
- ⁴⁸Hall, K. C., Thomas, J. P., and Dowell, E. H., "Proper Orthogonal Decomposition Technique for Transonic Unsteady Aerodynamic Flows," *AIAA Journal*, Vol. 38, No. 10, October 2000, pp. 1853–1862.
- ⁴⁹Florea, R., Hall, K. C., and Dowell, E. H., "Eigenmode Analysis and Reduced-Order Modeling of Unsteady Transonic Potential Flow Around Airfoils," *Journal of Aircraft*, Vol. 37, No. 3, May–June 2000, pp. 454–462.
- ⁵⁰Tang, D. M., Dowell, E. H., and Peters, D. A., "Reduced Order Aerodynamic Models Based Upon Inflow Eigenmodes," *Journal of the American Helicopter Society*, Vol. 43, No. 4, October 1998, pp. 342–351.
- ⁵¹Dowell, E. H., Hall, K. C., and Romanowski, M. C., "Eigenmode Analysis in Unsteady Aerodynamics: Reduced Order Models," *Applied Mechanics Reviews*, Vol. 50, No. 6, 1997, pp. 371–385.
- ⁵²Dowell, E. H., "Eigenmode Analysis in Unsteady Aerodynamics: Reduced-Order Models," *AIAA Journal*, Vol. 34, No. 8, August 1996, pp. 1578–1583.
- ⁵³Romanowski, M. C. and Dowell, E. H., "Aeroelastic Analysis of an Airfoil Using Eigenmode Based Reduced Order Unsteady Aerodynamics," AIAA Paper 95-1380.
- ⁵⁴Li, A. Q. and Dowell, E. H., "Modal Reduction of Mathematical Models of Biological Molecules," *Journal of Computational Physics*, Vol. 211, No. 1, January 2006, pp. 262–288.
- ⁵⁵Tang, D. M. and Dowell, E. H., "Reduced Order Model Analysis for Two-Dimensional Molecular Dynamic Chain Structure Attached to an Atomic Force Microscope," *Journal of Dynamic Systems Measurement and Control - Transactions of the ASME*, Vol. 126, No. 3, September 2005, pp. 531–546.
- ⁵⁶Tang, D. M., Li, A. Q., Attar, P. J., and Dowell, E. H., "Reduced Order Dynamic Model for Polysaccharides Molecule Attached to an Atomic Force Microscope," *Journal of Computational Physics*, Vol. 201, No. 2, December 2004, pp. 723–752.
- ⁵⁷Dowell, E. H. and Tang, D. M., "Multiscale, Multiphenomena Modeling and Simulation at the Nanoscale: On Constructing Reduced-Order Models for Nonlinear Dynamical Systems with Many Degrees-of-Freedom," *Journal of Applied Mechanics - Transactions of the ASME*, Vol. 70, No. 3, May 2003, pp. 328–338.
- ⁵⁸Attar, P. J. and Dowell, E. H., "A Reduced Order System ID Approach to the Modeling of Nonlinear Structural Behavior in Aeroelasticity," *Journal of Fluids and Structures*, Vol. 21, No. 5–7, December 2005, pp. 531–542.
- ⁵⁹Tang, D. M., Kholodar, D., Juang, J. N., and Dowell, E. H., "System Identification and Proper Orthogonal Decomposition Method Applied to Unsteady Aerodynamics," *AIAA Journal*, Vol. 39, No. 8, August 2001, pp. 1569–1576.
- ⁶⁰Hall, K. C., Thomas, J. P., and Clark, W. S., "Computation of Unsteady Nonlinear Flows in Cascades Using a Harmonic Balance Technique," *AIAA Journal*, Vol. 40, No. 5, 2002, pp. 879–886.
- ⁶¹Thomas, J. P., Dowell, E. H., and Hall, K. C., "Nonlinear Inviscid Aerodynamic Effects on Transonic Divergence, Flutter and Limit Cycle Oscillations," *AIAA Journal*, Vol. 40, No. 4, April 2002, pp. 638–646.